



Faculty of Manufacturing Engineering

**CHARACTERIZATION OF BROOKITE THIN FILM DEPOSITED
BY SPIN COATING METHOD WITH GREEN SOL-GEL ROUTE**



Nur Dalilah binti Johari

Doctor of Philosophy in Manufacturing Engineering

2022

DECLARATION

I declare that this thesis entitled “Characterization of Brookite Thin Film Deposited by Spin Coating Method with Green Sol-Gel Route” is the result of my own research except as cited in the references. The thesis has not been accepted for any degree and is not concurrently submitted in candidature of any other degree.


Signature :
Name : Nur Dalilah binti Johari
Date : 26/07/2022


اونيورسيتي تيكنيكل مليسيا ملاك
UNIVERSITI TEKNIKAL MALAYSIA MELAKA

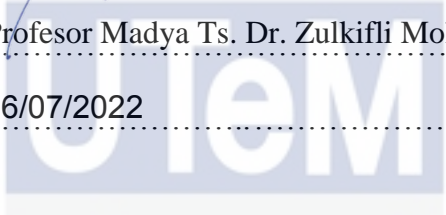
APPROVAL

I hereby declare that I have read this thesis and in my opinion this thesis is sufficient in terms of scope and quality for the award of Doctor of Philosophy.

Signature : 

Supervisor Name : Profesor Madya Ts. Dr. Zulkifli Mohd Rosli

Date : 26/07/2022



اونيورسيتي تيكنيكل مليسيا ملاك
UNIVERSITI TEKNIKAL MALAYSIA MELAKA

DEDICATION

To my beloved father and mother,
my husband and daughters,
my family and family in law,
my supervisor and my supportive friends that accompanying me along the difficult
pathway in my university life.



ABSTRACT

Brookite thin film is one of the great interests as a photocatalyst for water treatment in photocatalytic applications. Brookite has several advantages, but its applicability has been mainly limited because of the inability to synthesize brookite in pure phase due to its high purity and large surface area. One way to overcome such limitation is to establish the brookite phase by optimizing the synthesizing technique and sol-gel formulation. The current study was focused on the comparative deposition methods between dip and spin coating in order to evaluate the brookite phase. The green sol used was made free from solvent as an attempt for a green sol-gel route. The heat treatment temperature is varied and fixed at 200°C, 300°C, 400°C and 500°C for 3 h. The produced thin films were characterized by X-ray diffraction (XRD), Raman spectroscopy, scanning electron microscopy (SEM), transmission electron microscopy (TEM) and Fourier-transform infrared spectroscopy (FTIR). Results showed that deposition methods influence the type of phase formation and crystallinity. TiO₂ thin films via dip coating composed of anatase (101) at $2\theta = 25^\circ$ and rutile (110) at $2\theta = 27^\circ$ while spin coating produce single brookite (111) at $2\theta = 31^\circ$. The crystallite size of brookite thin film was larger (47.9 nm and 58.4 nm) compared to dip coating (5.0 nm to 28.8 nm). Raman shows that the TiO₂ thin film via dip and spin coating has a mixture of anatase, rutile and brookite. SEM analysis shows that the brookite thin film deposited via spin coating produced uniform and crack free coating at 200°C and 300°C. Brookite thin film had a crack coating with a width of 3.1 μm at 400°C and 1.5 μm at 500°C. In comparison to the TiO₂ thin film deposited via dip coating, which had a dense coating and cracks ranging in width from 0.4 μm to 4.3 μm . The coating thickness of brookite thin films via spin coating was in the range of 350.6 nm to 618.7 nm and TiO₂ thin films via dip coating was in the range of 320.5 nm to 1005.9 nm. TEM analysis on the films deposited via spin coating confirmed the presence of only brookite crystallites with lattice fringes of 0.28 nm compared to films via dip coating, which show anatase with lattice fringes of 0.35 nm and rutile with lattice fringes of 0.33 nm. FTIR results shows the TiO₂ thin film obtained via dip and spin coating contained the hydroxyl group on the surface of thin film. Next, the properties of brookite thin films via spin coating, which is band gap energy were in the range of 3.37 eV to 3.90 eV at 200°C to 500°C. The water contact angle of brookite thin films via spin coating was between 11.79° to 19.64° at 200°C to 500°C. The degradation of methylene blue shows the brookite thin film at 300°C and 200°C exhibit the highest degradation of methylene blue under UV light (67.7% and 63.0% after 4 h) and visible light (97.8% and 95.4% after 4 h) irradiation, respectively. The larger crystallite size (47.9 nm and 58.4 nm) and lower band gap energy value (3.37 eV) influenced the degradation of methylene blue. Thus, from the results, the brookite thin film coating was shown to be more effective in the degradation of methylene blue under visible light irradiation compared to under UV light irradiation in decomposing water contaminants by transforming them into benign substances.

PENCIRIAN FILEM NIPIS BROKIT DIENDAP OLEH KAEDAH PENYALUTAN BERPUTAR DENGAN LALUAN SOL-GEL HIJAU

ABSTRAK

Penyalutan filem nipis brokit sangat menarik sebagai permangkin untuk rawatan air dalam aplikasi fotopemangkinan. Terdapat pelbagai kelebihan Brokit, tetapi ianya terhad kerana ketidakmampuannya disintesis atas faktor ketulenannya yang tinggi dan luas permukaan yang besar. Salah satu cara untuk mengatasi perkara tersebut adalah dengan mewujudkan fasa brokit melalui pengoptimuman teknik sintesis dan formulasi sol-gel. Kajian semasa adalah memfokuskan kepada perbandingan kaedah endapan antara penyalutan celup dan penyalutan berputar bagi menilai fasa brokit. Sol hijau yang dihasilkan bebas daripada pelarut sebagai percubaan menghasilkan sol-gel hijau. Suhu rawatan haba dibezakan pada 200°C, 300°C, 400°C dan 500°C selama 3 jam. Pencirian filem nipis menggunakan pembelauan sinar-X (XRD), spektroskopi raman, mikroskop elektron imbasan (SEM), elektron penghantaran mikroskopik (TEM) dan spektroskopi Fourier-jelmaan inframerah (FTIR). Keputusan menunjukkan kaedah pengendapan mempengaruhi jenis pembentukan fasa dan penghabluran. Filem nipis TiO₂ dihasilkan melalui penyalutan celup yang terurai daripada anatas (101) di $2\theta = 25^\circ$ dan rutil (110) di $2\theta = 27^\circ$ manakala penyalutan berputar menghasilkan hanya brokit (111) di $2\theta = 31^\circ$. Saiz kristal filem nipis brokit adalah besar (47.9 nm dan 58.4 nm) berbanding penyalutan celup (5.0 nm hingga 28.8 nm). Raman menunjukkan filem nipis TiO₂ daripada penyalutan celup dan berputar mempunyai campuran anatas, rutil dan brokit. Analisis SEM pada filem nipis brokit melalui penyalutan berputar pada suhu 200°C dan 300°C, menunjukkan salutannya seragam dan tiada retakan. Pada suhu 400°C dan 500°C, terdapat retakan dengan lebar 3.1 μm dan 1.5 μm . Berbanding filem nipis TiO₂ melalui penyalutan celup, salutannya padat dan retakannya antara 0.4 μm hingga 4.3 μm . Ketebalan filem melalui penyalutan mejam adalah di antara 350.6 nm hingga 618.7 nm dan penyalutan celup adalah di antara 320.5 nm hingga 1005.9 nm. Analisis TEM untuk filem dimendapkan melalui penyalutan berputar mengesahkan kehadiran hanya kristal brokit dengan pinggir kekisi 0.28 nm berbanding filem melalui penyalutan celup yang pinggir kekisi anatas 0.35 nm dan pinggir kekisi rutil 0.33 nm. Keputusan FTIR menunjukkan filem nipis TiO₂ dihasilkan dari penyalutan celup dan berputar mengandungi kumpulan hidroksi pada permukaan filem. Seterusnya, sifat filem nipis brokit melalui penyalutan berputar mempunyai jurang tenaga di antara 3.37 eV hingga 3.90 eV. Sudut sentuh air filem nipis brokit melalui penyalutan berputar adalah di antara 11.79° hingga 19.64°. Degradasi metilena biru menunjukkan filem nipis brokit pada 300°C dan 200°C mempunyai degradasi metilena biru paling tinggi di bawah penyinaran cahaya UV (67.7% dan 63.0% selepas 4 jam) dan penyinaran cahaya nampak (97.8% dan 95.4% selepas 4 jam). Saiz kristal yang besar (47.9 nm dan 58.4 nm) dan jurang tenaga yang rendah (3.37 eV) mempengaruhi degradasi metilena biru. Oleh itu, salutan filem nipis brokit lebih berkesan pada degradasi metilena biru di bawah penyinaran cahaya nampak berbanding penyinaran cahaya UV dalam mengurai bahan cemar air.

ACKNOWLEDGEMENTS

I am grateful to Allah SWT for His grace, leading, and guidance, as well as for providing this opportunity to pursue my dream of completing a PhD in manufacturing engineering. First of all, I wish to express my gratitude and sincerely thank my supervisor, Associate Professor Ts. Dr. Zulkifli Mohd Rosli, for his advice and generous support and excellent guidance for me in completing this work. I would like to thank Associate Professor Dr. Jariah Mohamd Juoi for her constructive feedback and valuable comments on any possible improvements to my study.

I would like to acknowledge the support from Universiti Teknikal Malaysia Melaka (UTeM) and the Ministry of Higher Education, Malaysia through the grants FRGS/1/2014/TK04/FKP/02/F00215, FRGS/1/2016/TK05/FKP-AMC/F00319 and MyPhD (MyBRAIN15) for providing the opportunity and scholarship which enabled this research to be carried out. Besides, I would like to thank the staff of the Manufacturing Engineering Laboratory, Universiti Teknikal Malaysia Melaka (UTeM) for facilitating the equipment and machines for running the experiments.

Special thanks to all my colleagues and family who went through hard times together, cheered me on, and celebrated each accomplishment.

Thank you to my partner, Mohd Firdaus Aa'zami and my daughters for constantly listening to me rant and talk things out, for proofreading over and over, for cracking jokes when things became too serious, and for the sacrifices you have made in order for me to pursue my Ph.D.

TABLE OF CONTENTS

	PAGE
DECLARATION	
APPROVAL	
DEDICATION	
ABSTRACT	i
ABSTRAK	ii
ACKNOWLEDGEMENTS	iii
TABLE OF CONTENTS	iv
LIST OF TABLES	vii
LIST OF FIGURES	ix
LIST OF ABBREVIATIONS	xiii
LIST OF SYMBOLS	xv
LIST OF APPENDICES	xvii
LIST OF PUBLICATIONS	xviii
CHAPTER	
1. INTRODUCTION	1
1.1 Introduction	1
1.2 Background of Study	1
1.3 Problem Statement	5
1.4 Research Objective	8
1.5 Scope of Research	8
1.6 Thesis Outline	10
1.7 Summary	11
2. LITERATURE REVIEW	12
2.1 Introduction	12
2.1.1 Anatase	13
2.1.2 Rutile	15
2.1.3 Brookite	17
2.2 Brookite Characteristic and Its Properties	19
2.2.1 Crystal Structure	19
2.2.2 Morphology and Microstructure	27
2.2.3 Chemical Bonding	39
2.2.4 Electronic and Electrical Properties	43
2.2.5 Hydrophilicity Properties	46
2.3 Brookite Product Form	52
2.4 Sol-Gel Process	60
2.4.1 Sol-Gel Parameters	61
2.4.1.1 Titanium (IV) Isopropoxide as a TiO ₂ Precursor	61

2.4.1.2 Solvent and Solventless	64
2.4.1.3 Deionized Water	68
2.4.1.4 Hydrochloric Acid as a Catalyst	70
2.5 Deposition Method	72
2.6 Heat Treatment Temperature	81
2.7 Thin Film Photocatalytic Activity	84
2.8.1 Theory and Mechanism	86
2.8.2 Advantage and Application	89
2.9 Summary	90
3. METHODOLOGY	92
3.1 Introduction	92
3.2 Research Flowchart	92
3.3 Raw Materials	93
3.4 TiO ₂ Sol Preparation	94
3.5 Glass Substrate Preparation	96
3.5.1 Dip Coating Method	96
3.5.2 Spin Coating Method	97
3.5.3 Heat Treatment Temperature	98
3.6 Characterization and Analysis of the TiO ₂ Thin Film	99
3.6.1 X-ray Diffraction (XRD)	100
3.6.2 Raman Spectroscopy (RS)	102
3.6.3 Scanning Electron Microscopy (SEM), Cross Sectional Morphology and Energy Dispersive X-ray (EDX)	106
3.6.4 Transmission Electron Microscopy (TEM)	110
3.6.5 Fourier Transform Infrared (FTIR) Spectra	113
3.6.6 Ultraviolet-Visible Spectrophotometer (UV-Vis)	115
3.6.6.1 Band Gap Energy Measurement	117
3.6.7 Water Contact Angle Measurement	117
3.7 Photocatalytic Test	120
3.7.1 Methylene Blue (MB) Preparation	120
3.7.2 Degradation of Methylene Blue Dye	120
3.7.3 UV-Visible spectroscopy (UV-Vis)	121
3.8 Summary	122
4. RESULT AND DISCUSSION	123
4.1 Introduction	123
4.2 Characteristic of Green TiO ₂ Thin Films Deposited by Dip and Spin Coating	123
4.2.1 X-ray Diffraction (XRD)	123
4.2.2 Raman Spectroscopy (RS)	131
4.2.3 Scanning Electron Microscopy (SEM), Cross Sectional Morphology and Energy Dispersive X-ray (EDX)	138
4.2.4 Transmission Electron Microscopy (TEM)	147

4.2.5	Fourier Transform Infrared Spectroscopy (FTIR)	150
4.3	Effects of Deposition Method towards the Properties of Brookite Thin Film Coatings	152
4.3.1	Ultraviolet-Visible Spectrometer (UV-Vis)	153
4.3.2	Water Contact Angle Analysis of the Brookite Thin Film Coating	155
4.4	Photocatalytic Testing on Brookite Thin Film Coating	158
4.4.1	Degradation of Methylene Blue under UV Light Irradiation	158
4.4.2	Degradation of Methylene Blue under Visible Light Irradiation	160
4.4.3	Mechanism of Photocatalytic in Brookite Thin Film Coating	161
4.4.3.1	Effect of the Crystallite Size on Degradation of Methylene Blue	161
4.4.3.2	Effect of the Band Gap Energy on Degradation of Methylene Blue	162
4.5	Summary	164
5.	CONCLUSION AND RECOMMENDATION	165
5.1	Conclusion	165
5.2	Recommendation	167
	REFERENCES	168
	APPENDIX A	198



LIST OF TABLES

TABLE	TITLE	PAGE
2.1	X-ray diffraction (XRD) data for anatase (Verma et al., 2017)	14
2.2	X-ray diffraction (XRD) data for rutile (Verma et al., 2017)	16
2.3	X-ray diffraction (XRD) data for brookite(Verma et al., 2017)	18
2.4	Comparison on the brookite crystal structure and its characteristics. (D, crystallite size; E_g , band gap energy; θ , contact angle)	20
2.5	SEM images of the brookite powders and film for different process and temperature	29
2.6	TEM images of the brookite powder and film with different process preparation	34
2.7	Band gap energy values TiO_2 phase especially brookite	46
2.8	Contact angle value of the brookite film	48
2.9	Summary of the preparation of brookite powder gained in the existing research with previously stated in the literature	54
2.10	Summary of the preparation of brookite film gained in the existing research with previously stated in the literature	57
2.11	Summary of the types of precursor that used in formation of brookite film	62
2.12	Summary of the brookite film that deposited by dip and spin coating	79

3.1	The detailed information for the chemical or raw material used in this study	94
4.1	Percentage of TiO ₂ phase composition of the deposited TiO ₂ thin films via dip and spin coating with regard to heat treatment temperatures	130
4.2	Raman band position for the TiO ₂ thin film via dip coating	133
4.3	Raman band position for the TiO ₂ thin film coating via spin coating	135
4.4	Surface morphology SEM of the TiO ₂ thin films deposited via dip and spin coating at various heat treatment temperature	140
4.5	Cross sectional morphology of the TiO ₂ thin films deposited via dip and spin coating at various heat treatment temperatures	142
4.6	The water contact angle θ of the brookite thin film coatings	157



LIST OF FIGURES

FIGURE	TITLE	PAGE
2.1	Crystal structure of anatase TiO ₂ (Gupta and Tripathi, 2011)	14
2.2	Crystal structure of rutile TiO ₂ (Gupta and Tripathi, 2011)	16
2.3	Crystal structures of brookite TiO ₂ (Paola et al., 2013)	18
2.4	The FTIR of anatase, rutile and brookite powders. A, B, and R represent to anatase, brookite, and rutile, respectively (Li et al., 2007)	39
2.5	FTIR spectra of pure nanobrookite TiO ₂ thin films for variation water:AcAc volume ratios: (a) 1, (b) 0.5, (c) 0.25 (Arier and Tepehan, 2011)	40
2.6	The FTIR spectra of the TiO ₂ powders. (T2 = Brookite, T3 = Anatase, T5 = Rutile, T7 = Rutile dominant) (Liao et al., 2012)	41
2.7	FTIR spectra of brookite, anatase and rutile TiO ₂ nanoparticles created via facile chemical methods (Verma et al., 2017)	42
2.8	Absorption spectra of nanobrookite TiO ₂ films for different water:AcAc volume ratios (Arier and Tepehan, 2011)	44
2.9	The contact angle value for anatase, rutile and brookite films (Bellardita et al., 2011)	47
2.10	Plot of contact angle versus pre-treatment temperature for Activ	50

	(◦) and for glass (•) (Mills and Crow, 2008)	
2.11	Water contact angle of membranes with TiO ₂ nanoparticles produced with variation of temperatures (Fischer et al., 2017)	51
2.12	The development of the brookite product form	52
2.13	Orientation of adjacent surface water molecules (Huang et al., 2014)	70
2.14	Surface morphology of TiO ₂ film with the attendance of (a) HCl and (b) NaOH (Johari et al., 2017)	72
2.15	Schematic diagram of the formed network during sol-gel process with acid catalyst (A) and base catalyst (B) (Nisticò et al., 2017)	72
2.16	Deposition method by sol-gel process (Nguyen-Tri et al., 2018)	73
2.17	Phase diagram of TiO ₂ (Primo et al., 2011)	82
2.18	Overview of TiO ₂ -based photocatalytic applications	84
2.19	Electron from excites an electron from the valence band to the conduction band (Pelaez et al., 2012)	87
3.1	The flowchart for the overall procedure of the experiment	93
3.2	Flowchart of the TiO ₂ sol preparation	95
3.3	TiO ₂ sol after aging for 48 hours synthesized by green sol-gel route	95
3.4	The clear glass substrate used in this work	96
3.5	Precision single dip coater apparatus of TEFINI Model DP1000	97
3.6	Sysile TB-616 Spin Coater	98
3.7	The process of the thermal cycle	99
3.8	Raman spectra of anatase, rutile and brookite (Monai et al., 2017)	105

3.9	The schematic diagram of a SEM	109
3.10	The specimen holder for TEM analysis	110
3.11	The schematic diagram of TEM	112
3.12	The schematic diagram of the FTIR process	114
3.13	Diagram illustrating the band gap	116
3.14	Illustration of contact angles formed by sessile liquid drops on a smooth homogeneous solid surface (Yuan and Lee, 2013)	119
3.15	Schematic diagram of water contact angle measurement (Jasmee et al., 2018)	119
3.16	Schematic diagram of photocatalytic test for MB degradation	121
4.1	X-Ray Diffraction (XRD) patterns of the deposited TiO ₂ thin films produced via (a) dip and (b) spin coating at various heat treatment temperatures	127
4.2	Crystallite sizes of the deposited TiO ₂ thin films via (a) dip (b) spin coating with regard to heat treatment temperatures	129
4.3	EDX elemental mapping images on the cross sectional morphology of the TiO ₂ thin films deposited via dip coating at (a) 200°C, (b) 300°C, (c) 400°C and (d) 500°C	144
4.4	EDX elemental mapping images on the cross sectional morphology of the TiO ₂ thin films deposited via spin coating at (a) 200°C, (b) 300°C, (c) 400°C and (d) 500°C	146
4.5	TEM microstructures of the TiO ₂ thin films deposited via dip coating heated at 300°C, inset shows selected area electron diffraction (SAED)	148

4.6	TEM microstructures of the TiO ₂ thin films deposited via spin coating at (a) 200°C and (b) 300°C, inset shows selected area electron diffraction (SAED)	149
4.7	FTIR spectra of TiO ₂ thin films deposited via (a) dip and (b) spin coating heated at various heat treatment temperature	152
4.8	Optical absorption spectra of the brookite thin film coatings heated at various heat treatment temperature	153
4.9	Band gap energy of the brookite thin film coatings heated at various heat treatment temperature	155
4.10	Degradation efficiency of methylene blue (MB) under UV light irradiation for brookite thin film coating at different heat treatment temperature	159
4.11	Degradation efficiency of methylene blue (MB) under visible light irradiation for brookite thin film coating at different heat treatment temperature	161
4.12	Mechanism photocatalytic performance of brookite thin film coating	164

LIST OF ABBREVIATIONS

ASTM	-	American Society for Testing and Materials
BSE	-	Back-scattered electrons
CB	-	Conduction band
P25	-	Degussa
DEA	-	Diethanolamine
EDX	-	Energy Dispersive X-ray
FFT	-	Fast Fourier transform
FTIR	-	Fourier-transform infrared spectroscopy
IR	-	Infrared
ICDD	-	International Centre for Diffraction Data
JCPDS	-	Joint Committee on Powder Diffraction Standards
MB	-	Methylene blue
M	-	Molarity
PEG	-	Polyethylene glycol
RS	-	Raman spectroscopy
SEM	-	Scanning electron microscopy
SE	-	Secondary electrons
SAED	-	Selected area (electron) diffraction
SAXS	-	Small-Angle X-Ray Scattering
TDMAT	-	Tetrakis dimethylamino titanium
TTIP	-	Titanium (IV) tetraisopropoxide

TTB	-	Titanium tetrabutoxide
TEM	-	Transmission electron microscopy
UV	-	Ultra-violet
UV-Vis	-	Ultraviolet-Visible Spectrometer
VB	-	Valence band
WAXS	-	Wide-Angle X-Ray Scattering
XRD	-	X-ray diffraction
YSZ	-	Yttria-stabilized zirconia



LIST OF SYMBOLS

Å	-	Angstrom
θ	-	Contact angle
D	-	Crystallite size
°	-	Degree
°C	-	Degree celsius
eV	-	Electronvolt
h	-	Hour
μl	-	Microliter
μm	-	Micrometer
mg	-	Milligram
ml	-	Milliliter
mm/s	-	Millimeters per second
mTorr	-	Millitorr
M	-	Molarity
nm	-	Nanometer
ppm	-	Parts per million



cm^{-1}	-	Per centimeter
min^{-1}	-	Per minute
%	-	Percentage
rpm	-	Rotation per minute
s	-	Second
W	-	Watt



LIST OF APPENDICES

APPENDIX	TITLE	PAGE
A	Calculation of Percentage of TiO ₂ phase composition of the deposited TiO ₂ thin films via dip and spin coating with regard to heat treatment temperatures	198



LIST OF PUBLICATIONS

Journal

1. Johari, N.D., Rosli, Z.M. and Juoi, J.M., 2022. Effect of Heat Treatment Temperature on the Structural, Morphological, Optical and Water Contact Angle Properties of Brookite TiO₂ Thin Film Deposited Via Green Sol–Gel Route for Photocatalytic Activity. *Journal of Materials Science: Materials in Electronics*, 33, pp. 15143-15155.
2. Johari, N.D., Rosli, Z.M., Juoi, J.M. and Moriga, T., 2021. Heat Treatment Temperature Influence on the Structural and Optical Properties of Brookite TiO₂ Thin Film Synthesized Using Green Sol-Gel Route. *Journal of Advanced Manufacturing Technology (JAMT)*, 15(3).
3. Johari, N.D., Rosli, Z.M., Juoi, J.M. and Yazid, S.A., 2019. Comparison on The TiO₂ Crystalline Phases Deposited Via Dip and Spin Coating Using Green Sol–Gel Route. *Journal of Materials Research and Technology*, 8(2), pp. 2350-2358.
4. Shuhadah, A.Y., Rosli, Z.M., Juoi, J.M., Johari, N.D., Suzaim, F.H. and Moriga, T., 2018. Influence of Water and Precursor Molarity on the TiO₂ Thin Films Deposited from Solventless Sol-Gel. *Journal of Advanced Manufacturing Technology (JAMT)*, 12(1 (4)), pp.125-134.
5. Musa, M.A., Juoi, J.M., Rosli, Z.M., Johari, N.D. and Moriga, T., 2018. Effect of Degussa P25 Content on the Deposition of TiO₂ Coating on Ceramic Substrate. *Journal of Advanced Manufacturing Technology (JAMT)*, 12(1 (3)), pp.111-124.

Conferences paper

1. Yazid, S.A., Rosli, Z.M., Juoi, J.M. and Johari, N.D., 2018. Raman Spectroscopy and XRD Investigation on TiO₂ Sol-Gel Dip Coating Thin Films Synthesizes with and Without Solvents. In *MATEC Web of Conferences*, 150, p. 04007. EDP Sciences.
2. Johari, N.D., Mohd Rosli, Z., Juoi, J.M. and Musa, M.A., 2017. Influence of Catalyst in Synthesizing Brookite Thin Film Coating. In *Solid State Phenomena*, 264, pp. 5-8.
3. Johari, N.D., Mohd Rosli, Z., Juoi, J.M. and Musa, M.A., 2017. Influence of sol-gel pH and soaking time on the morphology, phases and grain size of TiO₂ coating. In *Solid State Phenomena*, 268, pp. 219-223. Trans Tech Publications Ltd.
4. Musa, M.A., Juoi, J.M., Mohd Rosli, Z. and Johari, N.D., 2017. Effect of Degussa P25 on the Morphology, Thickness and Crystallinity of Sol-Gel TiO₂ Coating. In *Solid State Phenomena*, 268, pp. 224-228. Trans Tech Publications Ltd.
5. Musa, M.A., Juoi, J.M., Mohd Rosli, Z. and Johari, N.D., 2017. Characterization of TiO₂ Coating Deposited on Ceramic Substrate. In *Solid State Phenomena*, 264, pp. 38-41. Trans Tech Publications Ltd.

CHAPTER 1

INTRODUCTION

1.1 Introduction

This chapter provides a quick overview of the introduction, which includes the background of study, problem statement, research objectives, scope of research, and thesis outline. The brookite TiO_2 has been the subject of study to seek an optimum quality brookite thin film coating for the photocatalytic activity under ultra-violet (UV) and visible light irradiation via green sol-gel route.

1.2 Background of Study

Today's fast global population growth and extensive industrialisation are mostly to blame for massive environmental degradation produced by a variety of hazardous waste and organic pollutants. Water pollution results from the continual release of organic pollutants such as dyes into water resources, which affects not only human health but also aquatic life in water bodies (Pedanekar et al., 2020). Also, increased colouring in residual waterways from sectors such as textiles, pharmaceuticals, plastics, and cosmetics has recently become a major health and environmental concern (Srinivasan and Viraraghavan, 2010). Based on the current Lancet Commission on Pollution and Health, water-borne illnesses cause about 1.8 million deaths globally. The colouring structure consists of aromatic rings, metallic and halide ions which has high toxicity and low biodegradability that is known as an organic compound (Chen et al., 2014; Sadeghzadeh-Attar, 2018). There are many techniques available to eliminate the organic compound such as biodegradation,